Received: *October 1, 2016*
Revised: *December 14, 2016*
Accepted: *December 20, 2016*
Published: *January 4, 2017*

18TH International Workshop on Radiation Imaging Detectors
3–7 July 2016,
Barcelona, Spain

Imaging study of a phase-sensitive breast-CT system in continuous acquisition mode

P. Delogu,[a,1] **B. Golosio,**[b] **C. Fedon,**[c] **F. Arfelli,**[c] **R. Bellazzini,**[d] **A. Brez,**[d] **F. Brun,**[e] **F. Di Lillo,**[f] **D. Dreossi,**[e] **G. Mettivier,**[f] **M. Minuti,**[d] **P. Oliva,**[g] **M. Pichera,**[d] **L. Rigon,**[c] **P. Russo,**[f] **A. Sarno,**[f] **G. Spandre,**[d] **G. Tromba**[e] **and R. Longo**[c]

[a] *Dipartimento di Scienze Fisiche, della Terra e dell'Ambiente, Università di Siena and INFN, sez. di Pisa, Presidio San Niccolò, Via Roma 56, Siena, I-53100 Italy*

[b] *Dipartimento di Fisica, Università di Cagliari and INFN, Sez. di Cagliari, Complesso Universitario di Monserrato, S.P. Monserrato-Sestu Km 0,700, Monserrato, CA, I-09042 Italy*

[c] *Dipartimento di Fisica, Università di Trieste and INFN, sez. di Trieste, Via Alfonso Valerio 2, Trieste, I-34127 Italy*

[d] *INFN sez. di Pisa and PiXirad Imaging Counters srl, Largo B. Pontecorvo 3, Pisa, I-56127 Italy*

[e] *Elettra sincrotrone Trieste S.C.p.A, s.s. 14-km 163.5 in AREA Science Park, Basovizza, Trieste, I-34149 Italy*

[f] *Dipartimento di Fisica "Ettore Pancini", Università di Napoli Federico II and INFN, Complesso Universitario di Monte S. Angelo, Ed. 6, Via Cintia, Napoli, I-80126 Italy*

[g] *Dipartimento di Chimica e Farmacia, Università degli Studi di Sassari and INFN, sez. di Cagliari, Via Vienna 2, Sassari, I-07100 Italy*

E-mail: pasquale.delogu@unisi.it

[1] Corresponding author.

doi:10.1088/1748-0221/12/01/C01016

Abstract: The SYRMA-CT project aims to set-up the first clinical trial of phase-contrast breast Computed Tomography with synchrotron radiation at the SYRMEP beamline of Elettra, the Italian synchrotron light source. The challenge in a dedicated breast CT is to match a high spatial resolution with a low dose level. In order to fulfil these requirements, the SYRMA-CT project uses a large area CdTe single photon counting detector (Pixirad-8), simultaneous algebraic reconstruction technique (SART) and phase retrieval pre-processing.

This work investigates the imaging performances of the system in a continuous acquisition mode and with a low dose level towards the clinical application. A custom test object and a large surgical sample have been studied.

Keywords: Computerized Tomography (CT) and Computed Radiography (CR); Pixelated detectors and associated VLSI electronics; X-ray detectors; X-ray radiography and digital radiography (DR)

Contents

1 Introduction

Breast Computed Tomography (breast-CT) is a promising alternative technique to conventional Digital Mammography (DM) and Digital Breast Tomosynthesis (DBT) for diagnosis of breast cancer. Breast-CT can produce 3D images without the inherent limitations of the DBT images [1]. However, the limited spatial resolution and the higher dose delivered to patients when compared to DM, have been regarded so far as a limitations for the medical practice of this technique [2]. Pilot clinical studies have been performed by a few research groups aiming to show the potential role of breast-CT in visualization and diagnostic evaluation of breast abnormalities [3–6].

In this context, synchrotron radiation (SR) shows great advantages respect to conventional X-ray tube radiation: the intense and monochromatic SR beam allows obtaining images with high quality (in terms of contrast to noise ratio) with a dose reduction, due to the absence of the low-energy spectrum component. Moreover, the peculiar geometric setups of a synchrotron beamline, where the sample can be placed far from both the source (tens of meters) and the detector (some meters), permit to exploit the phase-contrast effects.

The advantage of the phase-contrast technique to the breast imaging [7, 8] is that the soft tissues can be better differentiated than in the absorption-based imaging. Compared with absorption-based CT, X-ray Phase-contrast breast-CT (PCT) is sensitive to phase variations, which in soft tissues can be larger than the absorption ones.

PCT is under investigation in some synchrotron facilities with promising results [9, 10]. In particular the SYRMA-CT (SYnchrotron Radiation for Mammography-CT) project [10] aims to setup the first clinical study of PCT at the SYRMEP (SYnchrotron RAdiation for MEdical Physics) beamline of Elettra, the Italian synchrotron light source in Trieste.

In the SYRMA-CT project a high efficiency photon counting, direct detection X-ray imaging detector (Pixirad-8) is used [11]. Most remarkable advantages of this kind of detectors are: the signal to noise ratio (SNR) is Poisson dominated (no electronic noise) and a high efficiency thanks to great thickness of high Z semiconductor sensitive layer [12].

Specifically tuned pre-processing algorithms, developed for taking advantage of the phase contrast, and the state of the art of tomographic reconstruction methods are also crucial to maximize the image quality and minimize the dose.

In this paper some recent results are presented and discussed. The number of projections can be reduced increasing the speed of the rotator and consequently reducing the scan acquisition time when the detector is setting up for maximum frame rate. The fluence rate has to be increased to deliver a constant dose with reduced number of projections.

The reconstructions of the projections obtained in this continuous modality can have both the problem of the angular under-sampling artifacts and the continuous motion effects. A study of the dependence of the blurring on the number of acquired projection is presented here. A large *ex vivo* human sample including breast tissue has been acquired at a dose clinically acceptable; images were reconstructed applying the phase retrieval pre-processing.

2 Materials and methods

2.1 Patient room

SYRMA-CT project is carried out at the SYRMEP beamline [13] of the Elettra synchrotron light source (Trieste, Italy). The patient room is specifically designed for allowing both mammography and breast-CT examinations. The patient lies prone on a bed support that includes a hole through which the breast hangs without compression in case of CT. During a breast-CT exam the support rotates around a vertical axis and translated in the vertical direction after each rotation in order to cover a large breast volume. The rotations of the bed support occur continuously with constant angular speed.

2.2 X-ray source and dose evaluation

The work presented hereby has been carried out with the Elettra machine running at electron energy of 2.4 GeV in top-up mode with multibunch filling pattern. The X-ray radiation source is one of the bending magnets of the storage ring; a double-crystal Si(111) monochromator can provide a beam energy in the range 8.5–40 keV, with energy resolution $\Delta E/E = 2 \times 10^{-3}$. The beam cross-section at the detector is 210 mm (horizontal) $\times$ 3.6 mm (vertical, Gaussian-like shape). Data are collected at a photon energy of 38 keV with a maximum fluence rate of 10^7 photons $\times$ mm$^{-2} \times$ s^{-1}. The fluence rate can be reduced by means of aluminium filters of different thickness used as attenuators. The air-kerma evaluation is provided by two custom-made ionization chambers that have been calibrated with respect to the air-kerma standard chamber for low-energy X-rays by the Department of Ionizing Radiation Metrology of the National Agency for New Technologies, Energy and Environment (ENEA-INMRI, Casaccia, Roma, Italy). In order to estimate the Mean Glandular Dose (MGD) delivered to the sample, the measured air-kerma is multiplied by *ad hoc* coefficients obtained by a previous validated Monte Carlo code [14, 15].

2.3 Detector

A large area CdTe single photon counting imaging detector (Pixirad-8) is used. This is an 8 blocks system based on Pixirad-1 device [11] produced by PIXIRAD Imaging Counters s.r.l.. Pixirad-1

has a hybrid architecture, in which the sensor and the readout electronics (ASIC) are manufactured and processed separately and then coupled, with the *flip-chip bonding (bump-bonding)* technique. Pixirad-8 is manufactured placing side-by-side 8 basic blocks with a dead space between blocks of 3 columns. The pixel size is 60 μm and the global active area is about 250×25 mm^2. The detector is able to count the X-ray photons converted in each pixel of the CdTe sensor, in two counters. Each counter can be written while the other is read. This feature leads to the so-called Dead Time Free (DTF) modality where no events are lost over the whole acquisition time. This modality is essential in clinics where the loss of events implies a useless dose to patient. In DTF modality the maximum frame rate of Pixirad-8 is 30 fps. The detector has been preliminary characterized at the SYRMEP beamline with dedicated measurements for phase-contrast breast-CT [16–18].

2.4 Acquisition procedure

In our current setup the detector drives the timing. To acquire a CT scan with a specific delivered dose, firstly the necessary air-kerma is evaluated [15]. Then the fluence rate, the total time required and the frame rate are chosen to satisfy the air-kerma constrain accordingly with the source and detector characteristics. The scan acquisition starts when the angular speed of the patient support reaches a constant value. The projections are acquired for a complete 180° or 360° rotation. Due to laminar shape of the beam, only a volume of about 3 mm height can be scanned in one rotation. To image a larger volume, the above procedure has to be repeated after a vertical movement of the support.

2.5 Image pre-processing and reconstruction algorithms

A pre-processing procedure is applied to all acquired projections. Since the detector height (25 mm) is greater of the beam height (about 3 mm), an image crop is applied. This first step allows reducing the dimension of the images, in terms of total number of pixels, saving computing time in following processing phases. Then, a flat-field correction levels out the gain of the pixels and, at the same time, homogenize the beam shape. Finally the dead spaces between the 8 ASIC blocks of Pixirad-8 are "seamed" reconstructing the missing pixels with a bilinear interpolation.

Two reconstruction algorithms are used: a standard filtered back projection (FBP) algorithm and a simultaneous algebraic reconstruction technique (SART) algorithm. The SART algorithm, useful especially in case of angular under-sampling, has been successfully used in a wide range of CT applications [19–21] and has been described in a previous paper [10].

In order to exploit the phase information carried out by the projections, a phase retrieval filter following the Homogeneous Transport of Intensity (TIE-Hom) algorithm [10, 22] is applied prior to the actual reconstruction. The phase retrieval pre-processing was applied to the data sampled at 60 μm pixel size, even if the image was reconstructed with 120 μm pixel size, in order to maximize the effectiveness of the algorithm, which is based on edge-enhancement signals [10].

2.6 Samples specifications and projections workflow

The samples used in this work are:

- a home-made machined phantom from a polyoxymethylene (i.e. Delrin) cylinder of 100 mm diameter and 10 mm thick. The phantom has a central circular hole (50 mm diameter), 12

radial grooves and groups of circular holes of different diameters (0.5 mm–1.9 mm) arranged at different distances from the center (see figure 1);

- a surgical sample of breast tissue containing an infiltrating ductal carcinoma (of about 15 mm diameter), and some micro-calcifications. The sample dimensions are about 80 mm × 55 mm, 15 mm thickness.

Both samples were imaged with a rotation of 180° and 1200 projections were acquired, corresponding to an angular sampling of 0.15°. The reconstructions have cubic voxels with a side of 120 μm and the slice dimension is 1250 × 1250 pixels.

The Delrin phantom was used to evaluate the dependence of the blurring from the angular sampling when the projections are acquired with continuous motion.

A lower number of projections would cause, in principle, under-sampling artifacts depending on the shape and size of the details in the image. These artifacts can be partially corrected when iterative algorithms (e.g. SART) are used to reconstruct the images [10].

The continuous motion causes a different outcome: an averaging operation over the covered angle during the projections acquisition is performed, leading to a tangential blurring on the reconstruction. The tangential length where points are averaged can be written as $L_{\text{tang}} = r\Delta\varphi$ where r is the distance from the center of rotation and $\Delta\varphi$ is the angular aperture of the wedge in radians. The continuous motion effect is expected to clearly degrade the image when the tangential length becomes dominant respect to the intrinsic spatial resolution of the system. This effect is not corrigible using iterative algorithms.

In this experiment the MGD was 20 mGy. Since the detector has a linear response in time, we have resampled the projection of the test object, by summing:

- adjacent couples of projections, (600 projections, angular sampling of 0.3°);
- adjacent quadruplets of projections, (300 projections, angular sampling of 0.6°);
- adjacent sextets of projections, (200 projections, angular sampling of 0.9°).

Projections were then reconstructed with FBP and SART. No phase retrieval pre-processing was applied to the projections in this study. The comparison has been carried out in two selected regions, far from the rotation axis, of the reconstructed images. The selected regions are displayed in figure 1. We compare the region of 0.5 mm diameter holes (ROI 1, figure 1a) and the tangential and radial profiles extracted from the two circular 1.9 mm holes (ROI 2, figure 1b). The inner hole (called "A") is placed at 34 mm from the center, the outer hole (called "B") is located at 44 mm from the center (figure 1b).

The *ex vivo* sample was fixed in formalin and sealed in a vacuum bag. The work reported in this paper was carried out following the Directive 2004/23/EC of the European Parliament and of the Council of 31 March 2004 on setting standards of quality and safety for the donation, procurement, testing, processing, preservation, storage and distribution of human tissues. The images presented in this study were acquired in order to guide the pathologist in the localization of the lesions for the histological preparation, according to the standard procedures of the Pathology Unit of the Academic Hospital of Cattinara, Trieste University, accredited by JCI (Joint Commission International). The

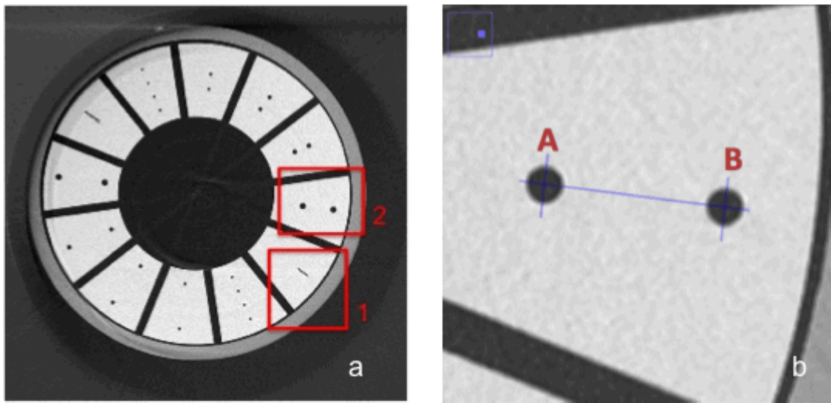

Figure 1. (a) A reconstructed slice of the Delrin phantom. The ROIs used for the comparison are shown. (b) Zoom of ROI 2 which show both the two holes (A and B) and the radial/tangential lines profile used.

sample was prepared from a specimen of breast lumpectomy and was derived from surgical material sent to the Pathology Unit according to local guidelines for histological examination. According to literature [23] the breast diameter (measured at the patient chest wall) is in the range 8–18 cm. Thus, the sample was lodged in a Plexiglas holder in order to replicate a mean breast diameter of 12 cm. Water was used to fill the space between holder and vacuum bag containing the sample. In such a way a medium-size dense breast was simulated. The MGD selected in this study for the breast phantom is 5 mGy.

To evaluate the improvement due to the phase information, we applied the phase retrieval algorithm for the breast phantom including the breast sample. Since the most important expected result is a reduction of the noise, we measured and compared the value of:

$$\frac{S}{N} = \frac{\langle I \rangle_{\mathrm{ROI}}}{\sigma_{\mathrm{ROI}}}$$

where $\langle I \rangle_{\mathrm{ROI}}$ is the mean pixel value and σ_{ROI} the standard deviation in a ROI. This quantity has been measured in homogeneous circular ROIs (corresponding to the filling water), with 1600 pixels area.

3 Results

Figure 2 shows the FBP reconstructions of the Delrin phantom at different angular sampling values. The detail is the ROI 1 of the figure 1. We observe an increasing blurring effect in the tangential direction, when angular sampling step grows and the number of projections decreases.

Figure 3 shows the tangential profiles of the holes in ROI 2 of figure 1b. The size of the holes is correctly estimated (the curves have the same FWHM) for all the angular sampling values, but the blurring of the edges (highlighted by the widening of the tails of the profiles) grows as the angular sampling value increases. This effect is independent on the reconstruction algorithm and is more important for the hole "B". This proves the relevance of the continuous motion effect that is greater for the hole "B" (since located faraway from the center with a larger L_{tang}). The blurring is pronounced in case of 200 and 300 projections and slight when switching from 1200 to 600 projections, where L_{tang} not yet dominates over the intrinsic spatial resolution.

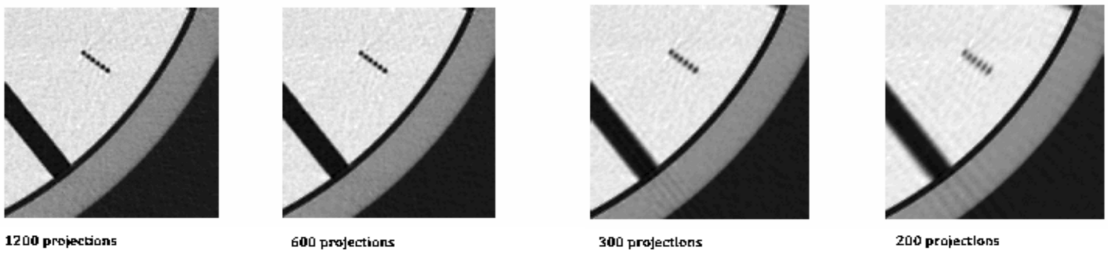

Figure 2. Detail of ROI1 showing the 0.5 mm holes reconstructed starting from different number of projections corresponding to increasing angular sampling.

Figure 4 shows the profiles of the holes "A" and "B" along the radius reported in figure 2b. The curves, corresponding to reconstructions of projection with different angular sampling, overlap.

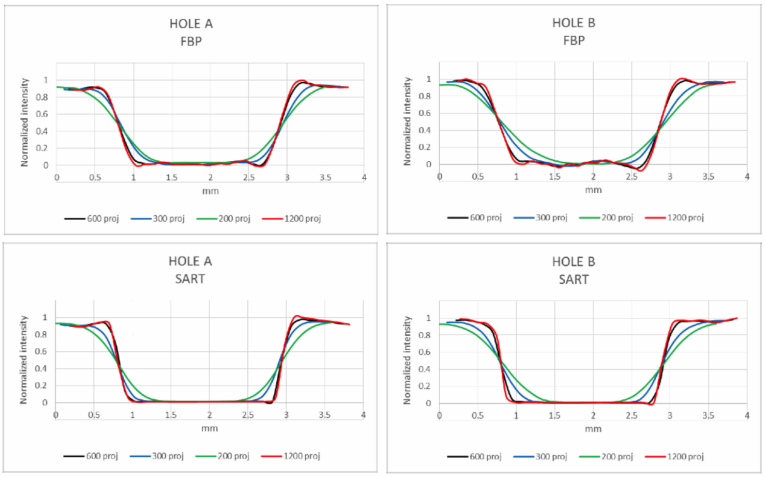

Figure 3. Tangential profiles of the two 1.9 mm diameter holes reported in figure 2b.

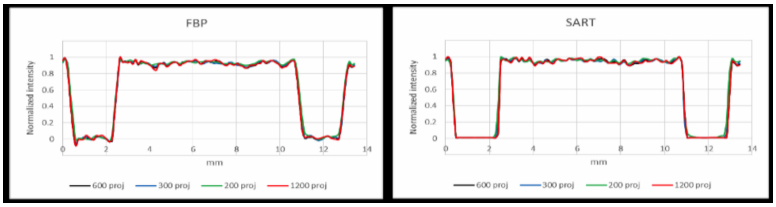

Figure 4. Radial profiles of the two 1.9 mm diameter holes.

Figure 5 shows the same slice of the breast sample without (a) and with (b) the phase retrieval. Both reconstructions show small and bright details (micro-calcifications). The outcome of the algorithm is the reduction of the noise without a visible drop in the spatial resolution.

In particular we measured:

- $\frac{S}{N} = 8.5 \pm 0.4$ in the image reconstructed without phase retrieval;
- $\frac{S}{N} = 21.6 \pm 1.5$ in the image reconstructed with phase retrieval.

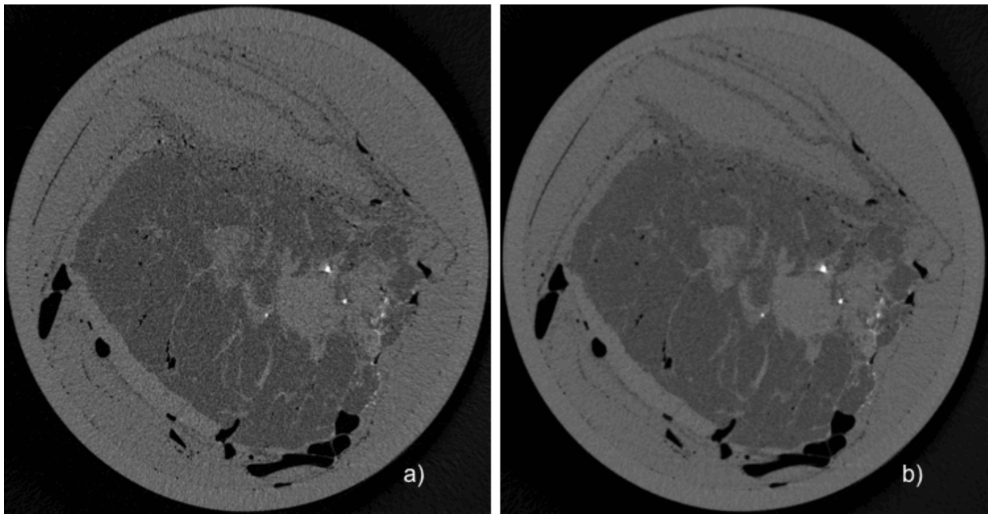

Figure 5. Reconstructions of the surgical sample without a) and with b) the application of the phase retrieval algorithm. The diameter is 12 cm (see text).

4 Conclusions

The development of a phase-sensitive CT system for breast imaging with synchrotron radiation, which fulfil the requirement of the breast-CT examination (e.g. low delivered dose and high spatial resolution) is a challenging task. The work hereby investigated several characteristics of the acquisition system setup towards the clinical study within the SYRMA-CT project. Thus, the angular sampling, the reconstruction modalities and the image quality are studied.

No relevant difference can be seen reducing the number of projection by half (see figure 3) in current experiment. However, this leads to a significant consequence on the exam as the necessary time can be halved. A scan time of 40 s is required to acquire a complete set of 1200 projections over 180 degrees at the maximum detector frame rate of 30 fps. The same frame rate can be kept to acquire 600 projections over 180 degrees in 20 s, due to the very high fluence rate available at the SYRMEP beamline.

Similar blurring effects are found both for SART and FBP reconstructions suggesting that the imaging degradation is rather due to continuous motion than to under-sampling. Further study are planned to better investigate the possible most favourable types of reconstruction algorithms.

The application of the phase retrieval algorithm improved the SNR of about 60% leading to a better visualization of the glandular structure. The microcalcification are very well detected even without the phase retrieved.

The results of this work contribute to better define the breast-CT protocol exam, which have to consider the dose constrained (i.e. comparable to the 5 mGy of DM) and the imaging quality.

Acknowledgments

The authors thank Fabrizio Zanconati for the sample preparation and Sara Savatovic for her help in the data analysis preparation.

This work was conducted within the SYRMA-CT project, which is funded by Istituto Nazionale di Fisica Nucleare (National Scientific Committee 5 for Technological and Inter-Disciplinary research) and supported by Elettra-Sincrotrone Trieste S.C.p.A. Christian Fedon is partially supported by Consorzio per la Fisica Trieste.

References

[1] A. Malliori et al., *Image quality evaluation of breast tomosynthesis with synchtron radiation*, *Med. Phys.* **39** (2012) 5621.

[2] W.A. Kalender et al., *High-resolution spiral CT of the breast at very low dose: concept and feasibility consideration*, *Eur. J. Radiol.* **22** (2012) 1.

[3] A. Sarno et al., *Dedicated breast computed tomography: Basic aspects*, *Med. Phys.* **42** (2015) 2786.

[4] N.D. Prionas et al., *Contrast-enhanced dedicated breast CT: initial clinical experience*, *Radiology* **256** (2010) 714.

[5] A.M. O'Connell et al., *The potential role of dedicated 3D breast CT as a diagnostic tool: review and early clinical examples*, *Breast J.* **20** (2014) 592.

[6] B. Zhao et al., *Cone beam breast CT with multiplanar and three dimensional visualisation in differentiating breast masses compared with mammography*, *Eur. J. Radiol.* **84** (2015) 48.

[7] P. Coan, A. Bravin and G. Tromba, *Phase-contrast x-ray imaging of the breast: recent developments towards clinics*, *J. Phys.* **D 46** (2013) e494007.

[8] E. Castelli et al., *Mammography with synchrotron radiation: first clinical experience with phase detection technique*, *Radiology* **259** (2011) 684.

[9] Y.I. Nesterets et al., *A feasibility study of X-ray phase-contrast mammographic tomography at the Imaging and Medical beamline of the Australian Synchrotron*, *J. Synchrotron Radiat.* **22** (2015) 1509.

[10] Longo et al., *Towards breast tomography with synchrotron radiation at Elettra: first images*, *Phys. Med. Biol.* **61** (2016) 1634.

[11] R. Bellazzini, G. Spandre, A. Brez, M. Minuti, M. Pinchera and P. Mozzo, *Chromatic X-Ray imaging with a fine pitch CdTe sensor coupled to a large area photon counting pixel ASIC*, 2013 *JINST* **8** C02028 [arXiv:1210.1248].

[12] K. Taguchi and J.S. Iwanczyk, *Vision 20/20: single photon counting x-ray detectors in medical imaging*, *Med. Phys.* **40** (2013) 100091.

[13] A. Abrami et al., *Medical applications of synchrotron radiation at the SYRMEP beamline of ELETTRA*, *Nucl. Instrum. Meth.* **A 548** (2005) 221.

[14] C. Fedon, F. Longo, G. Mettivier and R. Longo, *GEANT4 for breast dosimetry: parameters optimization study*, *Phys. Med. Biol.* **60** (2015) N311.

[15] G. Mettivier et al., *Glandular dose in breast computed tomography with synchrotron radiation*, *Phys. Med. Biol.* **61** (2016) 569.

[16] P. Delogu et al., *Characterization of Pixirad-1 photon counting detector for X-ray imaging*, 2016 *JINST* **11** P01015.

[17] A. Vincenzi et al., *Energy characterization of Pixirad-1 photon counting detector system*, 2015 *JINST* **10** C04010.

[18] A. Sarno et al., *Imaging performance of phase-contrast breast computed tomography with synchrotron radiation and a CdTe photon-counting detector*, *Phys. Med.* **32** (2016) 681.

[19] M.C. Camerani et al., *X-ray fluorescence tomography of individual municipal solid waste and biomass fly ash particles*, *Anal. Chem.* **76** (2004) 1568.

[20] B. Golosio, A. Brunetti and R. Cesareo, *Algorithmic techniques for quantitative Compton tomography*, *Nucl. Instrum. Meth.* **B 213** (2004) 108.

[21] J. Cauzid et al., 3*D imaging of vapour and liquid inclusions from Mole Granite, Australia, using helical fluorescence tomography*, *Spectrochim. Acta* **B 62** 799.

[22] D. Paganin et al., *Simultaneous phase and amplitude extraction from a single defocused image of a homogeneous object*, *J. Microsc.* **206** (2002) 33.

[23] S.Y. Huang et al., *The characterization of breast anatomical metrics using dedicated breast CT*, *Med. Phys.* **38** (2011) 2180.